

Dynamical correlations in dense metastable fluids

J. Ullo

Schlumberger-Doll Research, Old Quarry Road, Ridgefield, Connecticut 06877-4108

Sidney Yip

Department of Nuclear Engineering, Massachusetts Institute of Technology, Cambridge, Massachusetts 02139

(Received 19 July 1988)

Molecular-dynamics simulation results on soft-sphere fluids are presented that show the systematic changes in the equation of state, pair distribution function, self-diffusion coefficient, and various time-correlation functions with density at constant temperature in the metastable density region beyond the normal liquid range. At a characteristic density in this region, a decrease in the compressibility is observed along with a change in the density variation of the self-diffusion coefficient and the onset of a slowly decaying component in the density-correlation function. We interpret these behaviors as manifestations of a transition in which the particle dynamics changes its basic character, from collisions among particles undergoing continuous fluidlike displacements to barrier hopping of individual particles trapped in local-potential-energy minima. It is also concluded that this transition is distinct from the glass transition that occurs at a higher density.

I. INTRODUCTION

When fluids are rapidly cooled or compressed beyond the freezing point, the system can go into a metastable state characterized by long structural relaxation times. Information about atomic motions in such states on the molecular length and frequency scales is of interest in the study of supercooled liquids and glassy systems. In particular, detailed knowledge of how these motions affect the kinetics of relaxation and transport phenomena is essential to understanding the nature of the fluid-to-glass transition.¹⁻⁴

Molecular-dynamics simulation is a well-established method of studying the details of atomic motions in fluids.^{5,6} Using various model potentials for the interatomic interactions, simulations of supercooled and compressed fluids have provided information about thermodynamic and structural properties, transport coefficient data, and behavior of time-correlation functions in metastable systems.⁷⁻¹⁷ Further interest has stemmed from recent theoretical developments in self-consistent mode-coupling approximations, which appeared to have uncovered a mechanism for an ergodic-nonergodic transition which in turn may serve as a model for the liquid-to-glass transition.^{2,4,18-28} Since simulation can be performed using the potential function for which the mode-coupling calculations are tractable, a test of the theory in this respect is more direct by simulation than by experiments.

In this paper we describe a molecular-dynamics study in which a fluid system of particles interacting through purely repulsive forces described by a truncated Lennard-Jones potential is compressed to various densities at constant temperature. The purpose of our work is to determine the systematic variations in the structural and dynamical properties with density in the metastable region of density characteristic of supercooled liquids.

We believe that the present results, in contrast to simulations of quenching at constant pressure, are more amenable to physical interpretation and theoretical analysis since the effects observed can be attributed entirely to density changes.

When the fluid is compressed into the metastable density region, we observe from the variation of pressure a decrease in the compressibility factor which suggests the presence of a structural transition. Around the transition density the pair distribution function shows no significant changes and the self-diffusion coefficient is found to be still quite appreciable. In terms of time-correlation functions, there is the appearance of a slowly decaying mode in the density-correlation function and similarly in the Van Hove self-correlation function; on the other hand, the transverse-current correlation and the velocity-autocorrelation functions show the expected behavior of shear wave and damped vibrational modes, respectively, that are characteristic of dense fluids.

We regard the present results on equation of state, diffusion coefficient, and density-correlation functions as direct evidence of a transition which is dynamical in origin. Our interpretation is that the observed behaviors are manifestations of a change in the basic character of the many-body dynamics, from continuous collisions between particles with reduced but still liquid-like mobility to hopping motions of individual particles confined by local potential barriers. This change occurs in the metastable density region where the system properties are clearly distinct from those characteristic of glassy states. Its existence has implications concerning the feedback mechanism for particle localization treated in recent mode-coupling theory analyses.²⁶⁻²⁸

In Sec. II we describe the simulation model which is based on the Lennard-Jones interaction truncated at its minimum and the computational details of the simulation at constant volume and temperature. In Sec. III the re-

sults obtained at various densities along two isotherms are discussed in order: equation of state, radial distribution functions, mean-squared displacements and self-diffusion coefficients, density-and Van Hove self-correlation functions, velocity-autocorrelation functions, and the transverse-current correlations. In Sec. IV we conclude that our results provide evidence of a dynamical transition which, in the view of other recent finding, appears to be a general phenomenon of supercooled liquids, and we also discuss its implications concerning the self-consistent mode-coupling theories of dense fluids.

II. ISOTHERMAL COMPRESSION

We employed a standard molecular-dynamics technique for simulating fluid systems in the (N, V, E) ensemble. A system of $N=500$ particles interacting through the Lennard-Jones potential

$$V(r) = 4\epsilon[(\sigma/r)^{12} - (\sigma/r)^6] \quad (1)$$

is used with periodic boundary conditions. For computational savings the potential is truncated at $r=2^{1/6}\sigma$, so the particles interact only through purely repulsive forces. The particle trajectories are calculated using the Gear fifth-order predictor-corrector algorithm. To equilibrate at a given density-temperature state, the system volume is kept constant and the temperature is controlled by rescaling the particle velocities at every time step. Equilibrium is considered to be achieved if the temperature does not drift when rescaling is turned off. Typically, a run extends over 10^4 time steps for equilibration, followed by 2×10^4 steps for generating the trajectories for property calculations. All the simulation results will be reported in dimensionless units, energy is measured in ϵ length in σ , and time in $\tau = (m\sigma^2/\epsilon)^{1/2}$. The time-step in this unit is $\Delta t = 0.005\tau$. We also define the dimensionless density $n^* = n\sigma^3$, pressure $p^* = p\sigma^3/\epsilon$, and temperature $T^* = k_B T/\epsilon$.

We have carried out two series of simulations, one at $T^*=1.3$ and the other at $T^*=0.6$, with densities varying from $n^*=0.884$ (triple point density of a Lennard-Jones fluid) and below, up to $n^*=1.24$, which is 0.806 of hexagonal close packing. The higher temperature was initially chosen for the sake of comparison with mode-coupling-theory results appropriate to a hard-sphere system. However, it was found that the thermal motions contributed significantly to the onset of crystallization as the fluid was compressed; consequently a lowered temperature was chosen and most of the data reported here were obtained at $T^*=0.6$.

At each temperature the series was initiated at the lowest density and compression was carried out by scaling all the particle positions by an appropriate factor.²⁹ Normally the system configuration obtained at the end of a previous run was used for the next-higher-density run; however, at high compression, nucleation set in frequently and to avoid this it was necessary to use as a starting configuration that which was obtained at a density several steps lower. The criterion used for detecting nucleation was the presence of the second-nearest-neighbor peak in the radial distribution function $g(r)$. Recently,

Honeycutt and Anderson³⁰ have found that the critical nucleus may be already formed before the second-neighbor peak appears in $g(r)$. It is possible that some of the runs reported here would show crystallization behavior if the simulations had continued further. At least for the duration of the simulation we believe the fluids were in metastable states. At $T^*=0.6$ a few runs also were made by expanding the fluid. These results help to establish the reproducibility of the compression runs.

III. SIMULATION RESULTS

We begin with the equation-of-state results to delineate the density region where a transition appears to take place. Figure 1 shows the variation of pressure, calculated without the long-range correction, with density at the two temperatures. It can be seen that p^* is essentially piece-wise linear in n^* ; with increasing n^* there is a gradual transition to a larger value of dp^*/dn^* . At $T^*=0.6$ [Fig. 1(b)] this decrease in compressibility occurs at $n^*=1.02$, the intersection of the two asymptotes. We will refer to this density as n_x^* , the subscript x denoting a

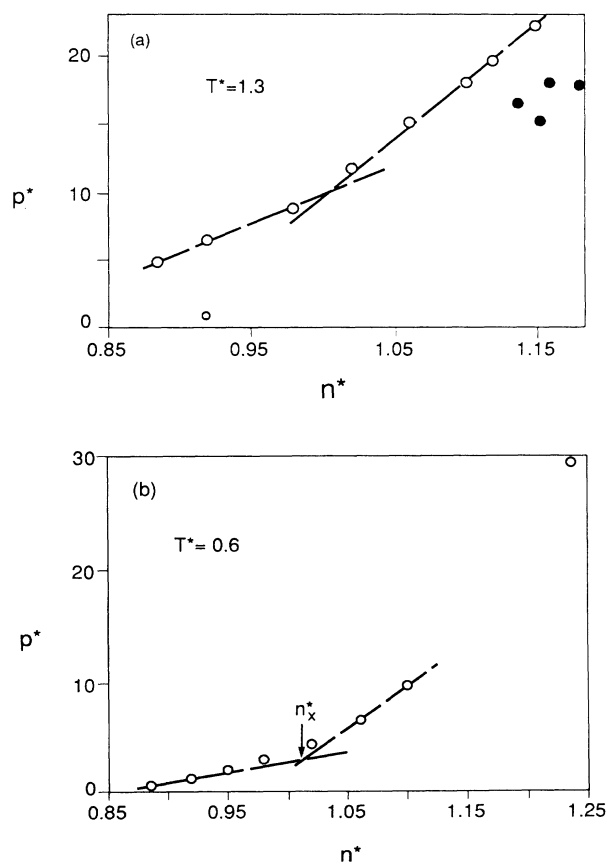


FIG. 1. Pressure-density variation along an isotherm; (a) $T^*=1.3$ and (b) $T^*=0.6$. Intersection of asymptotes can be used to define a transition density. Closed circles in (a) are obtained from simulations where nucleation is believed to have set in.

crossover transition.³ For $T^* = 1.3$, $n_x^* \approx 1.01$ [Fig. 1(a)].

In a simulation study of isobarically supercooled Lennard-Jones fluids, Fox and Anderson¹¹ found linear variation of n^* with T^* in two temperature regions, and a "glass transition" point was defined as the intersection of extrapolations from the linear regimes. Among the transition points thus obtained, a value of $n^* = 1.03$ was found at $T^* = 0.6$ and $p^* = 10$. Although our equation-of-state data indicate a transition around $n^* = 1.02$, we will refrain from calling it a glass transition. As we will see below, the diffusivity and various time-correlation functions are not what one would expect of a glass.

It should be noted that the system pressure is a sensitive indicator of crystallization during the simulation. The onset of nucleation gives rise to a significant drop in pressure, as can be seen in Fig. 1.

Figure 2 shows the $g(r)$ results for several densities. One sees the expected evolution from a typical liquid structure at the triple-point density $n^* = 0.884$ to a distri-

bution with a double peak at the position of second-nearest neighbor in the liquid, the characteristic signature of dense random packing.³¹ In Fig. 2(b) the $g(r)$ at $n^* = 1.02$ shows only a gradual flattening at the top of the second peak, otherwise there is nothing to correlate with the compressibility change in Fig. 1. In our $g(r)$ results the absence of a peak at $r^* \approx 2$, the position of second-nearest neighbor in an fcc lattice, is taken to be evidence that nucleation has not intervened. This criterion correlates quite well with the pressure drop. Thus, when the $g(r)$ shows this characteristic feature [$n^* = 1.17$ and 1.18 in Fig. 2(a)], one finds also a pressure decrease in Fig. 1.

Figure 3 shows the mean-squared displacement function

$$\langle \Delta r^2(t) \rangle = \frac{1}{N} \sum_j [\mathbf{r}_j(t) - \mathbf{r}_j(0)]^2, \quad (2)$$

where $\mathbf{r}_j(t)$ is the position of particle j at time t . If

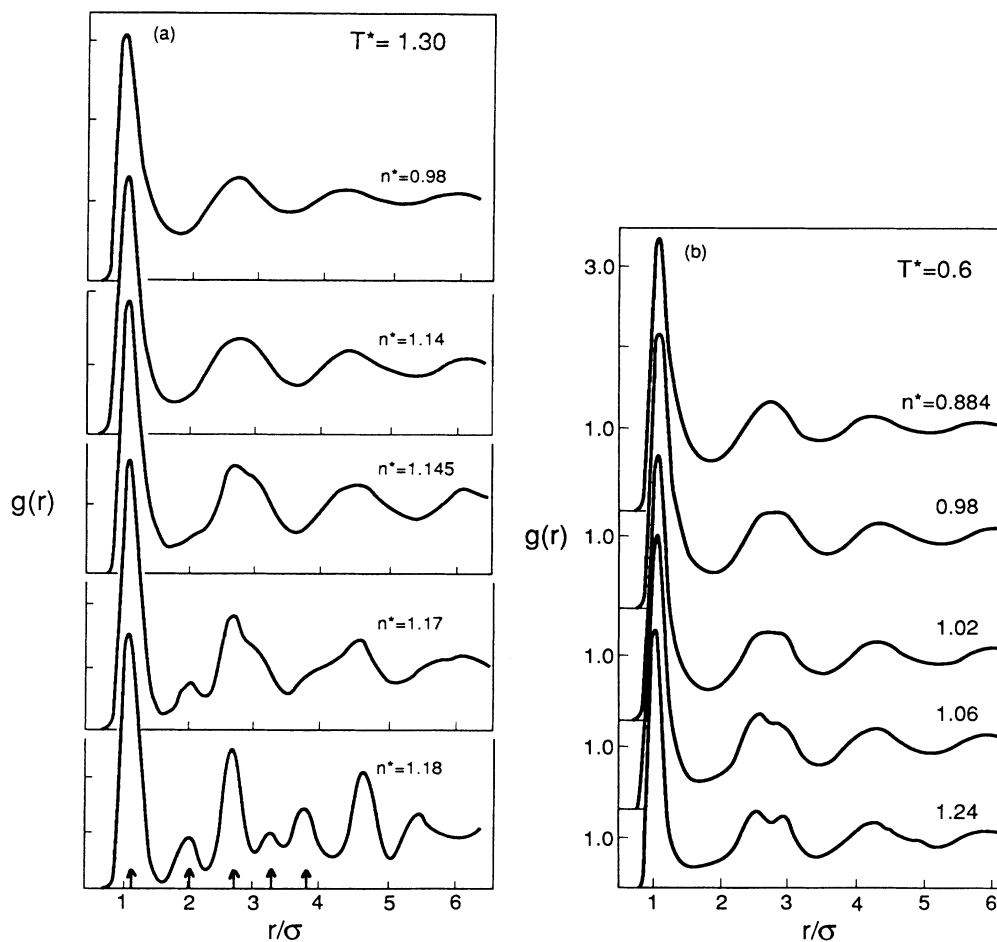


FIG. 2. Change in the radial distribution function with increasing density along an isotherm, (a) $T^* = 1.3$ and (b) $T^* = 0.6$. In (a) nucleation is believed to have set in at the two highest densities. The arrows indicate the positions of the first five nearest neighbors in a fcc lattice.

diffusive motion is occurring on the time scale of simulation, $\langle \Delta r^2 \rangle$ will exhibit a linear time variation with a slope equal to $6D$, D being the self-diffusion coefficient. This behavior is commonly observed in simulations of simple liquids where D typically has a value of 10^{-5} cm²/s. Using the potential parameters appropriate to argon this would correspond to the dimensionless diffusivity $D^* = D\tau/\sigma^2 = 0.0164$. In the present highly compressed fluids, atomic mobility is expected to be greatly restricted. As can be seen in Fig. 3, within the interval of simulation, a linear temporal variation characteristic of diffusion is quite clearly obtained for $n^* \leq 0.98$. For the next group densities [Fig. 3(b)] the temporal behavior is seen to be increasingly erratic. Also the observed magnitude of the root-mean-squared displacement becomes only comparable or less than the interatomic separation at these densities. One may regard these as in-

dicators of the onset of metastability. Although we will continue to extract a value for the self-diffusion coefficient for these densities, we should keep in mind that the results are less well determined. At $n^* = 1.24$ [Fig. 3(c)] $\langle \Delta r^2 \rangle$ is reduced by another order of magnitude. One can still observe an increase, but it is no longer justified to derive D from this behavior.

Figure 4 shows how the diffusion coefficients obtained from Fig. 3 vary with density. The data follow an essentially linear variation up to about $n^* = 0.98$, then gradually change over to a much slower decrease. If one extrapolates linearly to zero diffusivity in the low-compression region one obtains a value of $n^* = 1.01$, about the same density where a change in compressibility is observed (cf. Fig. 1). The value of D at $n^* = 1.02$ makes it seem unlikely that the fluid is in any state of significant structural arrest. Previous results obtained for hard-sphere fluids³²

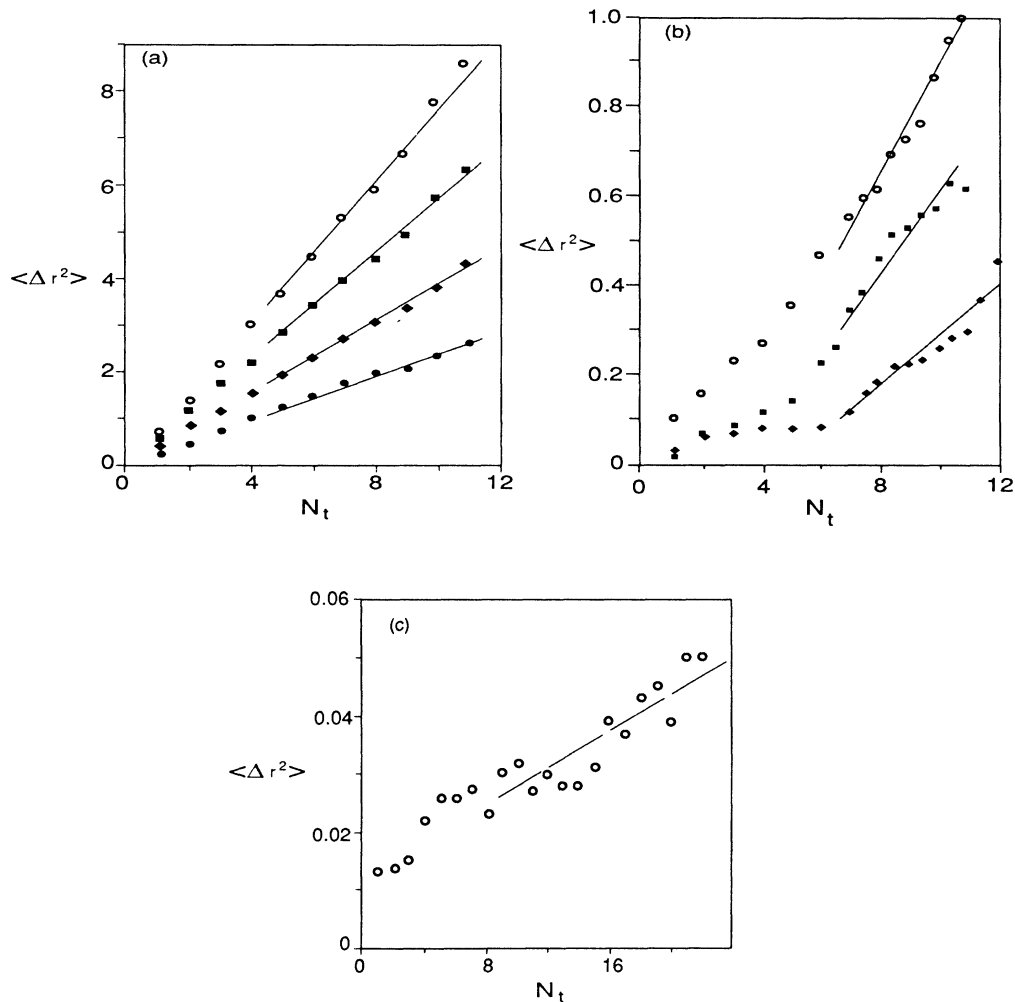


FIG. 3. Time variation of mean-squared displacement at various densities with $T^* = 0.6$: (a) $n^* = 0.884$ (open circles), 0.92 (squares), 0.95 (diamonds), 0.98 (closed circles); (b) $n^* = 1.02$ (open circles), 1.06 (squares), 1.10 (diamonds); and (c) $n^* = 1.24$. Straight lines indicate an attempt to extract a self-diffusion coefficient D from the slope.

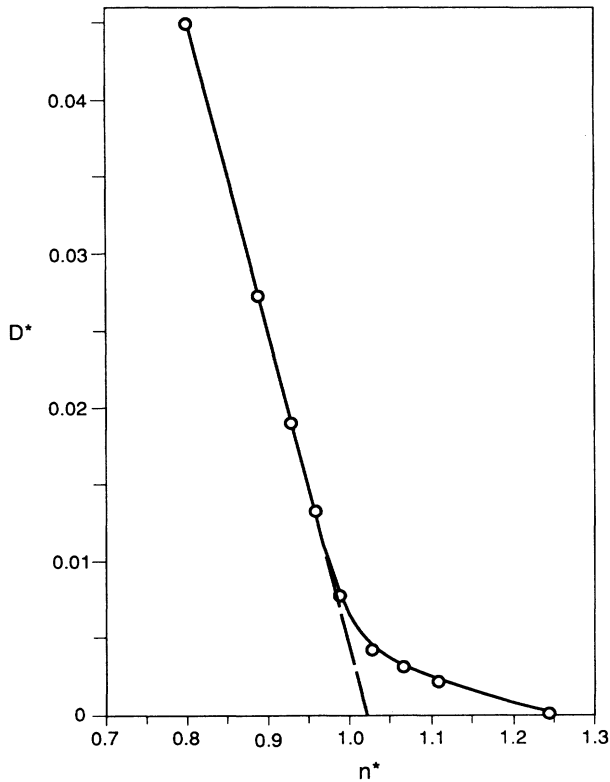


FIG. 4. Variation of diffusivity $D^* = D\tau/\sigma^2$ with density n^* at $T^* = 0.6$.

in a similar density region are found to follow an exponential behavior such as that prescribed by the Doolittle expression $D^*(V) \approx D_0 \exp[-A/(V - V_0)]$. It appears that a similar fit could also describe our data, although we feel that there are not enough points here to justify such a fit. Notice that according to the Doolittle expression, the diffusivity vanishes at a volume V_0 and the fit to the hard-sphere data gave a density $n^* \approx 1.24$ corresponding to V_0 .

On the basis of the diffusion data one can say that in the crossover region around n_x atomic diffusivity in the compressed fluid is sufficiently appreciable that it is inappropriate to associate the changes that occur with a glass transition. The fact that D^* goes over to an exponential type of volume variation does suggest the onset of a different type of dynamical process, possibly jump motions in the presence of an activation barrier as opposed to continuous displacements mixed with collisions with near neighbors.

In view of the foregoing data, it is interesting to see if the density-correlation function

$$F(\mathbf{k}, t) = \frac{1}{N} \sum_{i,j} \langle \exp\{i\mathbf{k} \cdot [\mathbf{r}_i(t) - \mathbf{r}_j(0)]\} \rangle \quad (3)$$

reveals any further information about the region of metastable states. Since $F(\mathbf{k}, t)$ should depend only on the magnitude of \mathbf{k} , it is necessary to evaluate Eq. (3) for a particular \mathbf{k} vector and then average the result over a

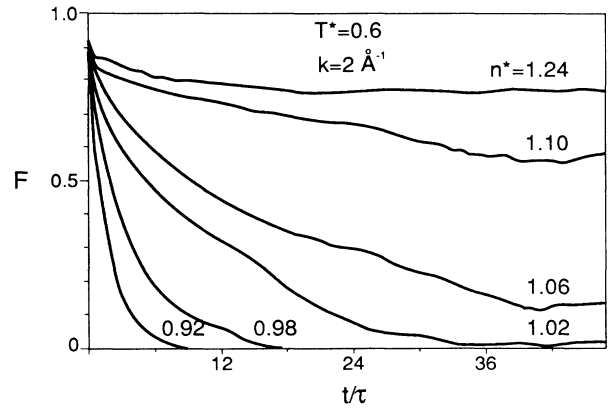


FIG. 5. Temporal decay of density fluctuations at wave number $k = 2 \text{ \AA}^{-1}$ obtained from simulations at various densities and $T^* = 0.6$. Time unit τ is defined as $(m\sigma^2/\epsilon)^{1/2}$.

number of equivalent \mathbf{k} vectors. We have used \mathbf{k} vectors in different directions having the same magnitude, and to enhance the statistics we also take other \mathbf{k} vectors with approximately the same (to within about 10%) magnitude. The results for $T^* = 0.6$ and $k = 2 \text{ \AA}^{-1}$ are shown in Fig. 5. In the interval in which we are able to observe the fluctuations, the decay of the density-correlation function extends to longer times as compression is increased. Around $n^* \approx 1.02$ there is the appearance of a slowly decaying component, possibly a behavior signifying the onset of structural arrest. At high compressions such as $n^* \geq 1.10$ the decomposition of $F(\mathbf{k}, t)$ into a fast decaying and a slow decaying component becomes quite evident; also the former appears to be insensitive to density changes. Given the limited time interval of the present simulations, one can only speculate about the behavior of $F(\mathbf{k}, t)$ at longer times. In particular, we cannot say whether $F(\mathbf{k}, t)$ follows a stretched exponential decay, as has been predicted by mode-coupling theory²⁷ and ob-

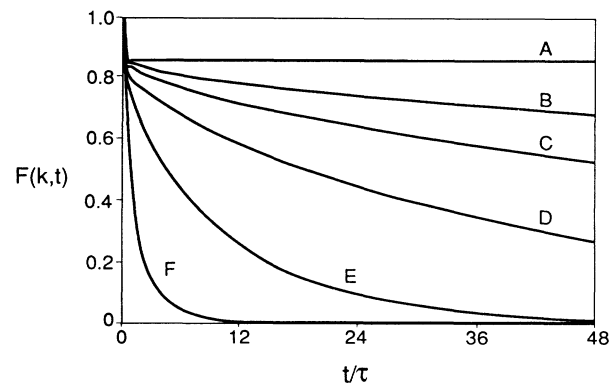


FIG. 6. Temporal decay of density fluctuations at reduced wave number $k\sigma = 7.0$ calculated by the self-consistent mode-coupling approximation for $T^* = 0.6$ at densities $n^* = 1.099$ (A), 1.094 (B), 1.088 (C), 1.072 (D), 1.043 (E) (Ref. 24). Curve F is for the triple point, $n^* = 0.884$ and $T^* = 0.722$.

served by neutron scattering.³³

Since the density-correlation function is the central quantity in the formulation of self-consistent mode-coupling theory,^{18,19} a direct comparison of calculation and simulation results on $F(k,t)$ is clearly desirable. The numerical calculations of Bengtzelius²⁴ are shown in Fig. 6, which is in the same form as Fig. 5. Although the density values are not the same from one figure to another, one should make note of the similarity between the theory and the simulation; in particular, the separation of the fast and slowly decaying components is seen to occur at about the same time and the same value of the correlation function. The main discrepancy revealed in this comparison lies in the high-compression regime. The highest density curve in Fig. 5 is at $n^*=1.24$, yet its time decay is intermediate to the behavior of the mode-

coupling results at $n^*=1.094$ and 1.099. We interpret the discrepancy to arise at least partly from the neglect of the coupling to current modes in the original version of the formulation.²⁴ Based on a simplified calculation²⁶ one knows that the time decay of $F(k,t)$ is more rapid when the current coupling is taken into account; this is also physically reasonable since additional coupling should result in greater dissipation. Thus we conclude that mode-coupling calculations with only coupling to density modes will overestimate the effect of structural arrest, and that numerical results derived from a more extended treatment^{26,27} will be in closer agreement with simulation.

Since freezing affects both collective and single-particle modes of motion, it is of interest to see how the Van Hove self-correlation function

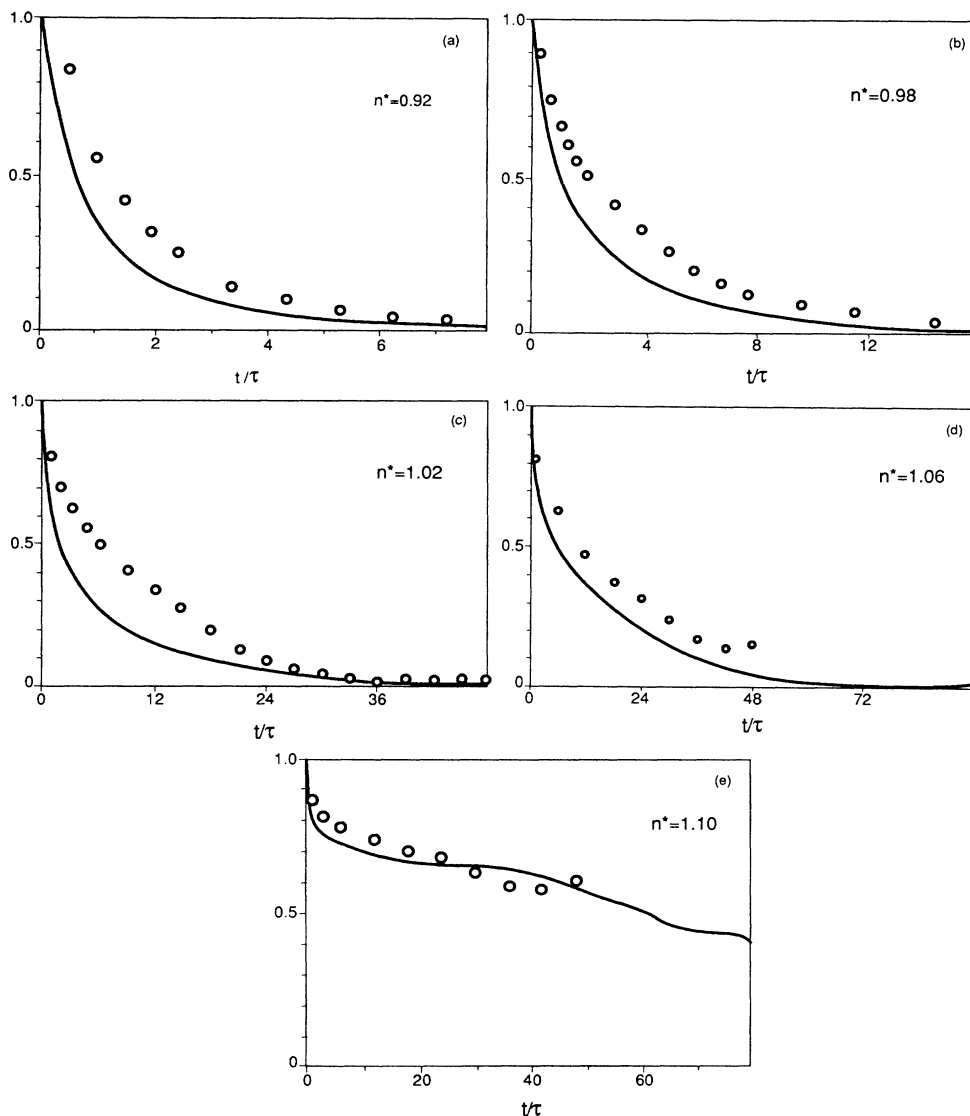


FIG. 7. Comparison of the temporal decays of the self-correlation function $F_s(k,t)$ (solid curves) and the density-correlation function $F(k,t)$ (circles) at $k = 2 \text{ \AA}^{-1}$ and $T^* = 0.6$. (a) $n^* = 0.92$, (b) $n^* = 0.98$, (c) $n^* = 1.02$, (d) $n^* = 1.06$, and (e) $n^* = 1.10$.

$$F_s(k, t) = \frac{1}{N} \sum_j \langle \exp\{i\mathbf{k} \cdot [\mathbf{r}_j(t) - \mathbf{r}_j(0)]\} \rangle \quad (4)$$

behaves. Figure 7 shows a comparison of $F(k, t)$ and $F_s(k, t)$. So far as the slowly decaying component is concerned, there is not much difference between the two correlation functions. The most striking difference is seen in the intermediate time region where the fluctuations involving the collective modes decay at a slower rate compared to fluctuations involving only single-particle motions. This difference will show up in the dynamic structure factors $S(k, \omega)$ and $S_s(k, \omega)$ in the frequency domain accessible by neutron scattering. Based on our results one would expect that the width of the quasielastic peak would be greater for incoherent scattering than for coherent scattering.

Thus far we have considered only density fluctuations at wavelengths corresponding to the diffraction maximum. This choice of k value is not meant to imply that the effects of freezing or structural arrest can be observed only at certain wavelengths. In Fig. 8 we show the self-correlation function at three different k values. One sees that the intensity of fluctuations is more strongly attenuated the higher the k value, otherwise there is nothing special in the k dependence of the self-correlation function. In $F(k, t)$ one can expect the onset of hydrodynamic behavior at $k \leq 1 \text{ \AA}^{-1}$; this should manifest itself mostly in the intermediate time region $\tau \leq 20\tau$. We show in Fig. 9 a few typical $S(k, \omega)$ at longer wavelengths. A heavily damped collective mode (sound waves) can be seen in these spectra.

We next consider another single-particle property, the velocity-autocorrelation function

$$\psi(t) = \frac{\left\langle \sum_j \mathbf{v}_j(t) \cdot \mathbf{v}_j(0) \right\rangle}{\left\langle \sum_l \mathbf{v}_l(0) \cdot \mathbf{v}_l(0) \right\rangle} \quad (5)$$

The behavior of $\psi(t)$ for a Lennard-Jones fluid at the triple point is well known.³⁴ Here we are interested mainly

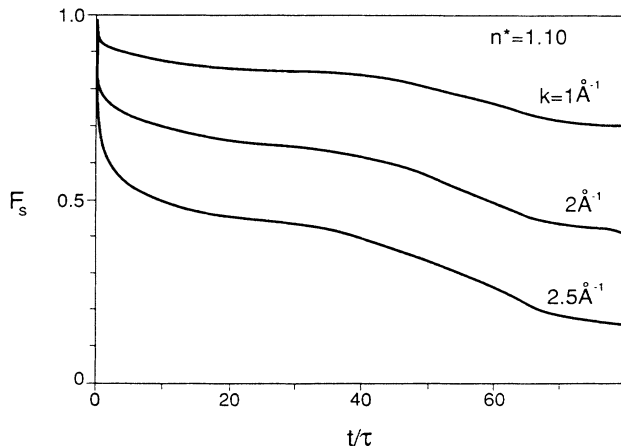


FIG. 8. Temporal decay of the self-correlation function $F_s(k, t)$ at $n^* = 1.10$, $T^* = 0.6$, and different wave numbers.

in how this function varies with increasing density. At the triple point, $\psi(t)$ decays to a negative value quite quickly, at about $t \approx 0.1\tau$, and with a few damped oscillations it goes to zero while remaining negative. This negative correlation reflects a strong cage effect provided by the neighboring atoms. However, the motion is not just one of simple rattling in a fixed cavity because $\psi(t)$ never becomes positive again. Figure 10(a) shows that the negative correlation is not seen at $n^* = 0.76$ because the density is not high enough. At $n^* = 0.84$ one has the typical behavior just described. The negative value of $\psi(t)$ is not as large as the full Lennard-Jones system because there are no attractive forces in the present simulation. With each density increase, $\psi(t)$ crosses zero at slightly earlier time and becomes more negative. The pattern holds even at $n^* = 1.10$. It is also interesting to note that $\psi(t)$ decays to zero in about the same time for all the densities shown.

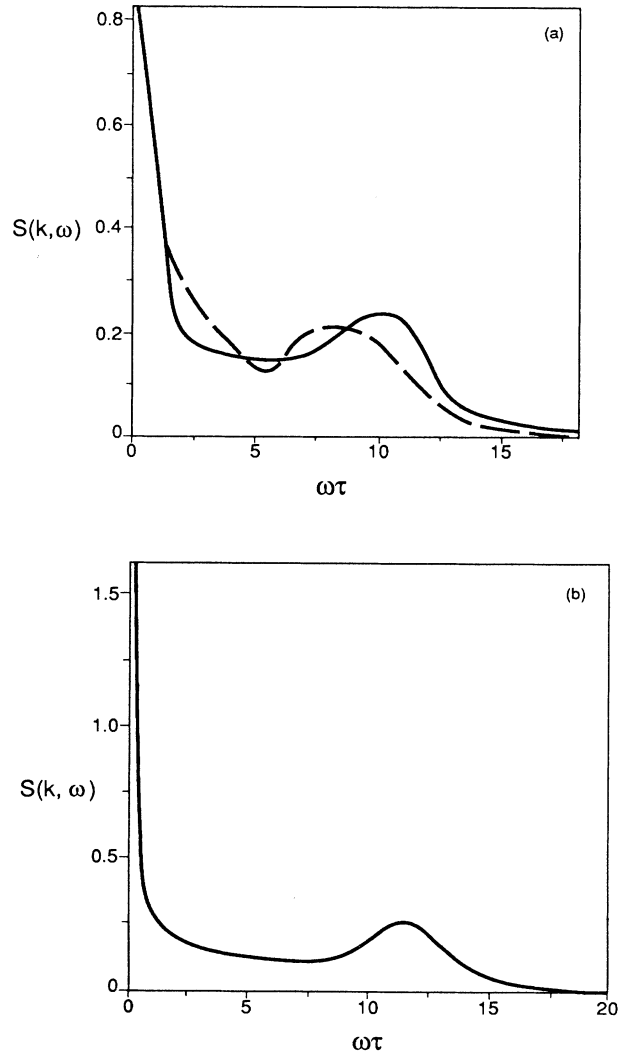


FIG. 9. Frequency spectrum of density fluctuations $S(k, \omega)$ at $k = 0.3 \text{ \AA}^{-1}$, $T^* = 0.6$: (a) $n^* = 0.95$ (dashed curve) and 0.98 (solid curve) and (b) $n^* = 1.02$.

The frequency spectrum

$$f(\omega) = \int_0^\infty \cos(\omega t) \psi(t) dt \quad (6)$$

shown in Fig. 10(b) reveals the distribution of vibrational frequencies at each density, with the zero-frequency value $f(\omega=0)$ being proportional to the self-diffusion coefficient. One sees that the presence of a negative region in $\psi(t)$ gives rise to a resonant mode at finite frequency in $f(\omega)$. At $n^*=1.10$ the value of $f(\omega=0)$ is just about at the limit of the statistical uncertainty of the data. It is doubtful that one can reliably extract D^* from the velocity-autocorrelation function data at densities beyond this [It is possible that the method of measuring the slope of $\langle \Delta r^2(t) \rangle$ may be used to somewhat higher density.] It is also of interest to comment on the shape of $f(\omega)$ at low frequencies. The slightly "convex" appearance of the distribution seems to be characteristic of an amorphous structure, in contrast to the ω^2 -like shape of a typical vibrational frequency distribution of an atomic lattice. This feature of $f(\omega)$ is discernible in neutron inelastic scattering data on metallic glasses.³⁵

Finally we consider the transverse-current correlation function

$$J_t(k, t) = \sum_{i,j} \langle [\mathbf{a} \cdot \mathbf{v}_i(t)] [\mathbf{a} \cdot \mathbf{v}_j(0)] \times \exp\{i\mathbf{k} \cdot [\mathbf{r}_i(t) - \mathbf{r}_j(0)]\} \rangle, \quad (7)$$

where \mathbf{a} is a unit vector perpendicular to \mathbf{k} . It is known that near the triple-point density $J_t(k, t)$ can decay to a negative value at short times, somewhat similar to the velocity-autocorrelation function. Physically this reflects

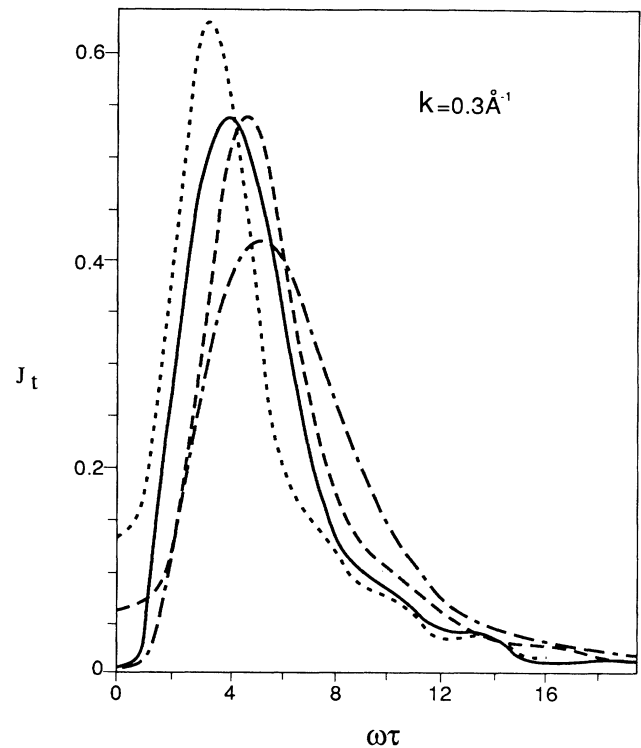


FIG. 11. Frequency spectrum of the transverse-current correlation function $J_t(k, \omega)$ at $k = 0.3 \text{ \AA}^{-1}$, $T^* = 0.6$, and various densities, $n^* = 0.98$ (dotted curve), 1.02 (solid curve), 1.06 (dashed curve), and 1.10 (dash-dotted curve).

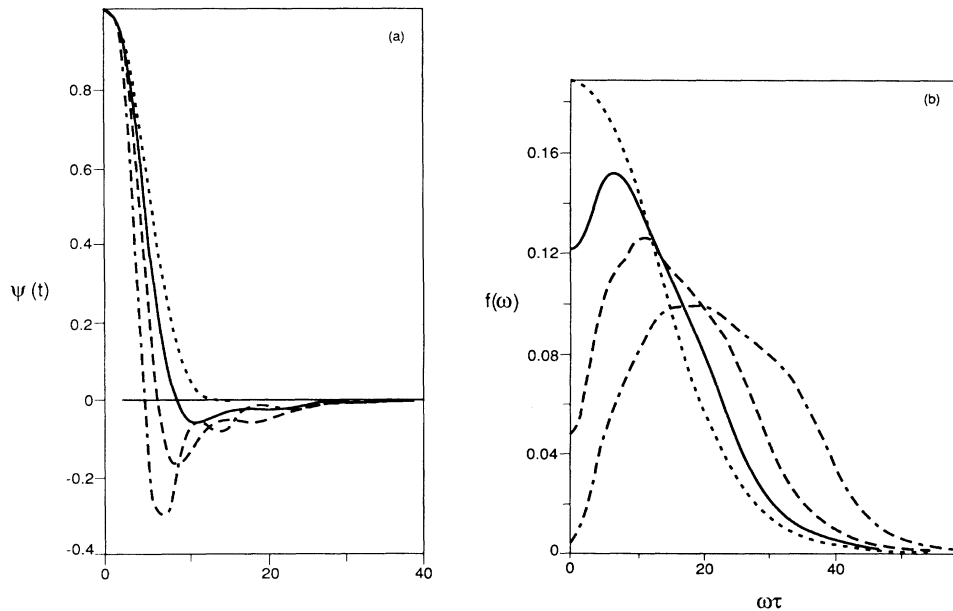


FIG. 10. Velocity-autocorrelation function $\psi(t)$ (a) and its frequency spectrum $f(\omega)$ (b) at $T^* = 0.6$ and various densities, $n^* = 0.76$ (dotted curve), 0.84 (solid curve), 0.95 (dashed curve), and 1.10 (dash-dotted curve).

the propagation of shear waves at finite wavelength in a fluid which exhibits viscoelastic behavior. Since a liquid cannot sustain any shear deformation, there is always a minimum value of k below which $J_i(k, t)$ will not become negative. Figure 11 shows the frequency spectra, the Fourier transform of Eq. (7), at $k=0.3 \text{ \AA}^{-1}$, the smallest k value that we can reach with the present size of simulation cell. The resonant mode, indicative of shear-wave excitation, is evident at all the densities shown; its peak position, which should be proportional to the high-frequency shear modulus, is seen to increase slightly with density. In the hydrodynamic limit, the zero-frequency value of $J_i(k, \omega)$ is proportional to the inverse viscosity. Thus at increasing compression, $J_i(k, \omega=0)$ should show a rapid decrease. Our data are not precise enough to enable a value of η to be extracted for $n^* > 1.02$. This is because $J_i(k, t)$ is sufficiently noisy at long times to require a cutoff before taking the Fourier transform, and statistical uncertainty associated with the cutoff makes it difficult to determine $J_i(k, \omega=0)$ with any accuracy when its intrinsic value is small. Another possible problem is that our k value may not be small enough for the full behavior of the hydrodynamic limit to set in. In any event we consider that the behavior of $J_i(k, t)$ is that of a viscoelastic fluid with nothing unusual occurring around $n^* = 1.02$.

IV. DISCUSSION

We have studied in this paper the systematic variation with density of equilibrium and time-correlation function properties of fluids in the metastable region. Although a truncated Lennard-Jones potential has been used, we believe that at these densities the results are not sensitive to the details of the potential. Therefore, our system can be regarded as a generic atomic fluid.

From the simulation results on the self-diffusion coefficient and the long-time decay of the density-correlation functions we conclude that a transition of dynamical origin occurs around a density which we called n_x^* . Our interpretation is that these results signal a gradual change in the fundamental character of the dynamical interactions, from continuous collisions among particles which still retain a certain degree of mobility to hopping over barriers by particles which find themselves being increasingly trapped in positions of local potential minima. It is also clear from the simulation results that this transition is distinct from the glass transition where the fluid is in a state of structural arrest with diffusivity still many orders of magnitude lower than those observed here.

While we have studied fluids only under compression, the results imply that for supercooled liquids there exists a corresponding transition at a characteristic temperature T_x which is distinctly above the glass transition temperature T_g .³ It is perhaps not surprising that among the many models and data interpretations of viscous liquids and the glass transition one finds arguments and discussions which contribute to the plausibility of such a transition; for example, from the point of view³⁶ that at low temperatures viscous flow is dominated by potential bar-

riers up to the point where significant fluidity sets in, a crossover transition³ would seem to be a natural consequence. There now exists experimental evidence to support this picture, as well as recent simulation and theoretical findings, to suggest that the crossover transition is a general phenomenon. From an analysis of shear viscosity data for a class of glass-forming liquids,³⁷ it is observed that upon supercooling the temperature variation of the viscosity above a characteristic temperature T_0 is noticeably different from its behavior at lower temperatures, and moreover, T_0 is considerably greater than T_g . From a molecular-dynamics study of local stress fluctuations in quenched liquids,³⁸ it is found that below a characteristic temperature T_s , which is well above T_g , the shear stresses become spatially correlated. From an analysis of spin-glass models,³⁹ it is shown that in such systems one can identify two transition temperatures, T_A and T_K , with $T_A > T_K$. At the former one has a dynamical transition which involves the onset of barriers in the local energy surface, and at the latter there is an equilibrium transition associated with the vanishing of the configurational entropy.

From the standpoint of dynamical descriptions of the liquid-to-glass transition, the extensions of the fluctuation hydrodynamics approach^{26,28} and the self-consistent mode-coupling approach²⁷ have both revealed a cutoff of the mechanism underlying the ergodic-to-nonergodic transition. As a result of including the coupling to current fluctuations, the density-correlation function is found to always decay to zero, although the decay rate is greatly reduced, and in the time region accessible to simulation there appears to be no qualitative difference in the behavior of $F(k, t)$.²⁶

Based on our results we believe that the cutoff mechanism is, in fact, an important effect, and the numerical calculations taking this into account⁴⁰ will bring the mode-coupling theory for the density-correlation function into closer agreement with simulation results such as those presented here. It appears that the ideal glass transition predicted by the original version of the theory^{18,19} is not observed in the present study. We may also conclude that, since none of the mode-coupling formulations thus far take into account dynamical processes of activated states, the transition temperature T_x represents the lower limit of applicability of these analyses. In view of the fact that the mode-coupling-theory approach is the only tractable quantitative description of time-correlation functions that can be used to analyze neutron⁴¹ and light⁴² scattering experiments, further investigations of this issue would of considerable interest.

ACKNOWLEDGMENTS

We have had helpful discussions with H. C. Anderson, C. A. Angell, U. Bengtzelius, S. P. Das, Y. Hiwatari, G. F. Mazenko, A. Sjolander, L. M. Torrell, P. Wolynes, and other colleagues. One of us (S.Y.) would like to acknowledge the support of the National Science Foundation under Grant Nos. CHE-8415078 and 8806767 and the hospitality of the Institute for Theoretical Physics, University of California, Santa Barbara.

- ¹For an overview, see Ann. N.Y. Acad. Sci. **484**, (whole volume) (1986).
- ²J. Jackle, Rep. Prog. Phys. **49**, 171 (1986).
- ³C. A. Angell, J. Phys. Chem. Solids **49**, 863 (1988).
- ⁴G. Frederickson, Ann. Rev. Phys. Chem. **39**, 149 (1988).
- ⁵See, for example, J.-P. Hansen and I. R. McDonald, *Theory of Simple Liquids*, 2nd ed. (Academic, New York, 1987); D. Tildesly and M. P. Allen, *Molecular Dynamics Simulations of Liquids* (Cambridge University Press, London, 1987).
- ⁶For a review of computer simulation of glasses, see C. A. Angell, J. H. R. Clarke, and L. V. Woodcock, Adv. Chem. Phys. **48**, 397 (1981).
- ⁷For first results on hard spheres, see L. V. Woodcock, J. Chem. Soc. Faraday Trans. 2 **72**, 1667 (1976); **74**, 11 (1978); Ann. N.Y. Acad. Sci. **371**, 274 (1981); see also J. M. Gordon, J. H. Gibbs, and P. D. Fleming, J. Chem. Phys. **65**, 2771 (1976).
- ⁸For first results on soft spheres, see Y. Hiwatari, J. Phys. Soc. Jpn. **47**, 733 (1979); J. Phys. C **13**, 5899 (1980); see also J. N. Cape and L. V. Woodcock, J. Chem. Phys. **72**, 976 (1980).
- ⁹For first results on Lennard-Jones particles, see A. Rahman, M. J. Mandell, and J. P. McTague, J. Chem. Phys. **64**, 1564 (1976); see also W. D. Kristensen, J. Non-Cryst. Solids **21**, 303 (1976); and J. H. R. Clarke, J. Chem. Soc. Faraday Trans. 2 **75**, 1371 (1979).
- ¹⁰M. Kimura and F. Yonezawa, in *Topological Disorder in Condensed Matter*, edited by F. Yonezawa and T. Ninomiya (Springer-Verlag, New York, 1983), p. 80.
- ¹¹J. R. Fox and H. C. Anderson, J. Phys. Chem. **88**, 4019 (1984).
- ¹²J. Ullo and S. Yip, Phys. Rev. Lett. **54**, 1509 (1985).
- ¹³J. G. Amar and R. D. Mountain, J. Chem. Phys. **86**, 2236 (1987).
- ¹⁴S. Kambayashi and Y. Hiwatari, J. Phys. Soc. Jpn. **56**, 2788 (1987).
- ¹⁵R. D. Mountain and D. Thirumalai, Phys. Rev. A **36**, 3300 (1987).
- ¹⁶B. Bernu, J. P. Hansen, Y. Hiwatari, and G. Pastore, Phys. Rev. A **36**, 4891 (1987).
- ¹⁷H. Miyagawa, Y. Hiwatari, B. Bernu, and J. P. Hansen, J. Chem. Phys. **88**, 3879 (1988).
- ¹⁸E. Leutheusser, Phys. Rev. A **29**, 2765 (1984).
- ¹⁹U. Bengtzelius, W. Götze, and A. Sjolander, J. Phys. C **17**, 5915 (1984). For further theoretical discussions and calculations, see Refs. 23 and 24, respectively.
- ²⁰T. R. Kirkpatrick, Phys. Rev. A **31**, 939 (1985).
- ²¹S. P. Das, G. F. Mazenko, S. Ramaswamy, and J. Toner, Phys. Rev. Lett. **54**, 118 (1985).
- ²²J. Bosse and J. S. Thakur, Phys. Rev. Lett. **59**, 998 (1987); U. Krieger and J. Bosse, *ibid.* **59**, 1601 (1987).
- ²³W. Götze, Z. Phys. B **56**, 139 (1984); Phys. Scr. **34**, 66 (1986); in *Amorphous and Liquid Materials*, edited by E. Luscher, G. Jacucci, and G. Fritsch (Nijhoff, Dordrecht, 1986); W. Götze and L. Sjogren, J. Phys. C **20**, 879 (1987).
- ²⁴U. Bengtzelius, Phys. Rev. A **33**, 3433 (1986); **34**, 5059 (1986).
- ²⁵T. R. Kirkpatrick and P. G. Wolynes, Phys. Rev. A **35**, 3072 (1987).
- ²⁶S. P. Das and G. F. Mazenko, Phys. Rev. A **34**, 2265 (1986).
- ²⁷W. Götze and L. Sjogren, Z. Phys. B **65**, 415 (1987).
- ²⁸S. P. Das, Phys. Rev. A **36**, 211 (1987).
- ²⁹For first simulations of fluid under compression, see F. F. Abraham, J. Chem. Phys. **72**, 359 (1980); L. V. Woodcock (Ref. 7); and J. H. R. Clarke, J. Chem. Soc. Faraday Trans. 2 **75**, 1371 (1979).
- ³⁰J. D. Honeycutt and H. C. Andersen, J. Phys. Chem. **91**, 4950 (1987).
- ³¹G. S. Cargill III, Solid State Phys. **30**, 227 (1975).
- ³²L. V. Woodcock and C. A. Angell, Phys. Rev. Lett. **47**, 1129 (1981).
- ³³F. Mezei, W. Knaak, and B. Farago, Phys. Rev. Lett. **58**, 571 (1987).
- ³⁴J. -P. Boon and S. Yip, *Molecular Hydrodynamics* (McGraw-Hill, New York, 1980).
- ³⁵J. B. Suck, H. Bretscher, H. Rudin, P. Grutter, and H. J. Guntherodt, Phys. Rev. Lett. **59**, 102 (1987).
- ³⁶M. Goldstein, J. Chem. Phys. **51**, 3728 (1969).
- ³⁷R. Tabor, R. N. Kleiman, and D. J. Bishop, Phys. Rev. B **34**, 1835 (1986).
- ³⁸S.-P. Chen, T. Egami, and V. Vitek, Phys. Rev. B **37**, 2440 (1988).
- ³⁹T. R. Kirkpatrick and D. Thirumalai, Phys. Rev. B **36**, 5388 (1987); see also **37**, 5342 (1988); and T. R. Kirkpatrick and P. J. Wolynes, *ibid.* **36**, 8552 (1987).
- ⁴⁰S. P. Das (private communication); (unpublished).
- ⁴¹See Proceedings of the Institute Laue-Langevin Workshop on Dynamics of Disordered Materials, Grenoble, 1988 (Springer-Verlag, New York, in press), and E. Y. Sheu, S. H. Chen, J. S. Huang, and J. C. Sung, Phys. Rev. A (to be published); see Ref. 33.
- ⁴²S. H. Chen and J. S. Huang, Phys. Rev. Lett. **55**, 1888 (1985); P. N. Pusey and W. van Megan, *ibid.* **59**, 2083 (1987); see also S. H. Chen, E. Y. Sheu, and J. S. Huang, in Ref. 41.